

Journal of Mechanical Engineering

An International Journal

Volume 10 No. 2

December 2013

ISSN 1823-5514

Simulation of Flow around a Flapping Wing
Using Two-dimensional Vortex Method

Akhmad Farid Widodo
Lavi Rizki Zuhail
Hari Muhammad

Material Characterization and Axial Crushing Tests of Single
and Double-Walled Columns at Intermediate Strain Rates

Leonardo Gunawan
Sahril Afandi Sitompul
Tatacipta Dirgantara
Ichsan Setya Putra
Hoon Huh

Stability Augmentation for Longitudinal Modes of a
Small Blended Wing-Body Aircraft with Canard
as Control Surface

Rizal E. M. Nasir
Wahyu Kuntjoro

Experimental Cooling Mode Variation of an
Air-Cooled Pem Fuel Cell Using Second-Order
Thermal Analysis

Wan Ahmad Najmi Wan Mohamed
Rahim Atan

Ballistic Resistance Analysis of Non-filled Tank
against Fragment Simulating Projectile (FSP)

MR. Aziz
W. Kuntjoro
NV. David
R. Ahmad

JOURNAL OF MECHANICAL ENGINEERING (JMeChE)

EDITORIAL BOARD

EDITOR IN CHIEF:

Professor Wahyu Kuntjoro – Universiti
Teknologi MARA, Malaysia

EDITORIAL BOARD:

Professor Ahmed Jaffar – Universiti
Teknologi MARA, Malaysia
Professor Bodo Heimann – Leibniz
University of Hannover Germany
Dr. Yongki Go Tiauw Hiong – Nanyang
Technological University, Singapore
Professor Mirosław L. Wyszynski –
University of Birmingham, UK
Professor Ahmad Kamal Ariffin Mohd Ihsan
– UKM Malaysia
Professor P. N. Rao, University of Northern
Iowa, USA
Professor Abdul Rahman Omar – Universiti
Teknologi MARA, Malaysia
Professor Masahiro Ohka – Nagoya
University, Japan
Datuk Professor Ow Chee Sheng – Universiti
Teknologi MARA, Malaysia
Professor Yongtae Do – Daegu University,
Korea
Dr. Ahmad Azlan Mat Isa – Universiti
Teknologi MARA, Malaysia
Professor Ichsan S. Putra – Bandung Institute
of Technology, Indonesia

Dr. Salmiah Kasolang – Universiti Teknologi
MARA, Malaysia
Dr. Mohd. Afian Omar – SIRIM Malaysia
Professor Darius Gnanaraj Solomon –
Karunya University, India
Professor Mohamad Nor Berhan – Universiti
Teknologi MARA, Malaysia
Professor Bernd Schwarze – University of
Applied Science, Osnabrueck, Germany
Dr. Rahim Atan – Universiti Teknologi
MARA, Malaysia
Professor Wirachman Wisnoe – Universiti
Teknologi MARA, Malaysia
Dr. Thomas Ward – University of Malaya,
Malaysia
Dr. Faqir Gul – Institute Technology Brunei,
Brunei Darussalam
Dr. Valliyappan David a/l Natarajan –
Universiti Teknologi MARA, Malaysia

EDITORIAL EXECUTIVE:

Dr. Koay Mei Hyie
Rosnadiyah Bahsan
Farrahshaida Mohd. Salleh
Mohamad Mazwan Mahat
Nurul Hayati Abdul Halim

Copyright © 2013 by the Faculty of Mechanical Engineering (FKM), Universiti Teknologi MARA, 40450 Shah Alam, Selangor, Malaysia.

All rights reserved. No part of this publication may be reproduced, stored in a retrieval system, or transmitted in any form or any means, electronic, mechanical, photocopying, recording or otherwise, without prior permission, in writing, from the publisher.

Journal of Mechanical Engineering (ISSN 1823-5514) is published by the Faculty of Mechanical Engineering (FKM) and UiTM Press, Universiti Teknologi MARA, 40450 Shah Alam, Selangor, Malaysia.

The views, opinions and technical recommendations expressed herein are those of individual researchers and authors and do not necessarily reflect the views of the Faculty or the University.

Journal of Mechanical Engineering

An International Journal

Volume 10 No. 2

December 2013

ISSN 1823-5514

- | | | |
|----|--|----|
| 1. | Simulation of Flow around a Flapping Wing Using Two-dimensional Vortex Method
<i>Akhmad Farid Widodo</i>
<i>Lavi Rizki Zuhul</i>
<i>Hari Muhammad</i> | 1 |
| 2. | Material Characterization and Axial Crushing Tests of Single and Double-Walled Columns at Intermediate Strain Rates
<i>Leonardo Gunawan</i>
<i>Sahril Afandi Sitompul</i>
<i>Tatacipta Dirgantara</i>
<i>Ichsan Setya Putra</i>
<i>Hoon Huh</i> | 19 |
| 3. | Stability Augmentation for Longitudinal Modes of a Small Blended Wing-Body Aircraft with Canard as Control Surface
<i>Rizal E. M. Nasir</i>
<i>Wahyu Kuntjoro</i> | 37 |
| 4. | Experimental Cooling Mode Variation of an Air-Cooled Pem Fuel Cell Using Second-Order Thermal Analysis
<i>Wan Ahmad Najmi Wan Mohamed</i>
<i>Rahim Atan</i> | 53 |

5. Ballistic Resistance Analysis of Non-filled Tank against Fragment
Simulating Projectile (FSP)

75

MR. Aziz

W. Kuntjoro

NV. David

R. Ahmad

Simulation of Flow around a Flapping Wing Using Two-dimensional Vortex Method

Akhmad Farid Widodo

Faculty of Mechanical and Aerospace Engineering

Bandung Institute of Technology

and

Laboratory of Aero-Gas dynamics and Vibration

The Indonesian Agency for Assessment and Application of Technology

Lavi Rizki Zuhail

Hari Muhammad

Faculty of Mechanical and Aerospace Engineering

Bandung Institute of Technology

ABSTRACT

In this work, two dimensional vortex method is developed and used to simulate flows around a flapping wing. The method solves Navier-Stokes equation in term of vorticity. The solving strategy is to split the equation into diffusion and convection terms, and solved them separately. The diffusion term is modelled by Particles Strength Exchange (PSE) which is the most accurate of diffusion modelling in vortex method. The convection term that represents transport of particles is calculated by time step integration of velocity. To exercise the capability of the method in handling complex flows, we carried out simulation of flow field around a flapping wing. The flapping cycle includes two strokes with rapid rotation near reversal stroke. The result demonstrates conformity of the simulation with experiment in revealing mechanism of force production due to wake capturing. The results also show spurious peaks of lift of simulation because of disappearance of vortex stretching.

Keywords: *Vortex Method, Particles Strength Exchange, Flapping Wing, Wake Capturing*

Introduction

Insects and birds have different mechanism than conventional airplane in producing aerodynamic lifting forces. They rely on kinematic of the wing motion, instead of the airfoil contour as in airplanes. The mechanism is so called 'flapping wing' phenomenon. It is really interesting because some insects or birds demonstrate effectiveness in producing lift and thrust impressively by employing the mechanism. This fact has triggered some researchers to investigate the aerodynamic mechanism of flapping force generation, which may be useful for designing flying robots.

Some numerical efforts have been conducted by some researchers to simulate flapping wing phenomena. They used various approaches to model the flow from the roughest approach based on potential flow like [1,2,3,4] to more complex flow models. The simple works were intended to investigate flapping force generated by inviscid flow. More advance modeling using Navier Stokes that have capability to capture viscosity effect have been carried out by [5,6,7].

An alternative method for simulating fluid flow based on Lagrangian approach named vortex method is expected to be the most suitable method for simulating flapping wing phenomena. It has some features that are advantageous for simulating flapping wing: mesh free simulation, inherently describing unsteadiness and fluid-viscosity dominated flow. The development of vortex method was pioneered by [8] who introduced solving strategy of vorticity equation in Lagrangian form by splitting diffusion-convection terms to be solved separately. The convection term which calculate evolution of particles position is obtained from velocity integration and the diffusion is approximated by random walk modelling. The random walk is roughest approximation of diffusion and then further contributions gave better kind of diffusion modelling. The major contributions can be mentioned here are core spreading [9] and particles strength exchange so called PSE introduced by [10]. The PSE is the most accurate approximation of diffusion but it suffers huge computational load.

This paper reports the application of vortex method using PSE diffusion for simulating cases representing flapping wing phenomena. The method is mainly contributed by [11]. The detail algorithm follows [12,13] that compile previous works [10,11,14,15]. The method has been utilized for moving body problem by [16,17]. The simulated cases follow Dickinson's experiment [18] who studied rotation effect of flapping wing. The work revealed the details of wake capturing process due to rotation, which is an important aspect that is responsible for generating lift. Although the experiment was three dimensional case, it is expected that the two dimensional numerical simulation can reproduce the main features revealed in the experiment.

Vortex Method

Governing Equation

The governing equation of vortex equation derived from Navier-Stokes equation in term of vorticity. For three dimensional problem is written as:

$$\frac{\partial \bar{\omega}}{\partial t} + \bar{\mathbf{u}} \cdot \nabla \bar{\omega} = \nabla \bar{\mathbf{u}} \cdot \bar{\omega} + \nu \nabla^2 \bar{\omega} \quad (1)$$

where $\bar{\mathbf{u}}(\mathbf{x}, t)$ is the velocity field, ν is the kinematic viscosity, t is time, and $\bar{\omega} = \nabla \times \bar{\mathbf{u}}$ is the vorticity. The Equation (1) can be interpreted physically as follows: the first term of the left hand side represents the unsteadiness of the flows. The second term of the left hand side represents the transport of vorticity in the flow due to velocity, that known as the convection term. In the right hand side, the first term represents the vortex stretching and the second is viscous diffusion. For two dimensional problem, vortex stretching is vanish so that the two dimensional governing equation is written as:

$$\frac{\partial \bar{\omega}}{\partial t} + \bar{\mathbf{u}} \cdot \nabla \bar{\omega} = \nu \nabla^2 \bar{\omega} \quad (2)$$

To solve numerically using standard finite difference method, the uniform grid is needed in computational domain. In vortex method, the diffusion term should be modeled with appropriate term to avoid the grid requirement.

Particles Blob Discretization

The vorticity equation (1) is solved in Lagrangian manner by discretizing flow field to be tracked by moving particles. The particles carry vorticity and convect with the local flow velocity. In the initial step of computation, the particles are arranged around geometry with the initial value of vorticity. The numerical computation of vortex method is to calculate the evolution of their vorticity and position as a function of time. The results of computation are vorticity and position of particles in time depended. During the computation, the vorticity field is represented by scalar value (for two dimensional) particles strength:

$$\omega(\mathbf{x}, t) = \sum_{i=1}^N \xi_i(\bar{\mathbf{x}} - \bar{\mathbf{x}}_i) \Gamma_i(\bar{\mathbf{x}}) \quad (3)$$

Where Γ_i is strength of particles and $\bar{\mathbf{x}}$ is vector of position with i is index of particles. A distribution function ξ_i describes distribution of vorticity in the blobs. Note that vorticity and strength of particles in two dimensional problem can be written as scalar instead of vector. Some distribution function have been introduced

to define the distribution [2,4] and we choose Gaussian distribution for robustness. Using the Gaussian, the distribution function can be defined as follow:

$$\xi_i(\mathbf{x}) = \frac{1}{2\pi\sigma_i^2} \exp\left(-\frac{1}{2}\left(\frac{|\mathbf{x}|}{\sigma_i}\right)^2\right) \quad (4)$$

With σ_i^2 represents the smoothing parameter. The strength of particles can be considered as accumulated vorticity of particles ‘blob’ in the core. If the particles have an area A_i , mathematically, the particles strength can be related to the vorticity as $\Gamma_i \triangleq \omega_i A_i$.

Method of Solution

Following the splitting scheme, the convection term of Equation (1) can be excluded and the rest is viscous problem that computes vorticity as a function of time. The convection term computes transport of particles by time step integration of velocity. The velocity is computed using Biot-Savart relation:

$$\mathbf{u}(\mathbf{x}_i, t) = - \sum \frac{q\left(\frac{|\bar{\mathbf{x}}_i - \bar{\mathbf{x}}_j|}{\sigma_j}\right)}{|\bar{\mathbf{x}}_i - \bar{\mathbf{x}}_j|^2} (\bar{\mathbf{x}}_i - \bar{\mathbf{x}}_j) \times \hat{\mathbf{e}}_z \Gamma_j \quad (5)$$

Where q for Gaussian distribution is defined as follow:

$$q(\rho) = \frac{1}{2\pi} \left(1 - \exp\left(-\frac{\rho^2}{2}\right)\right) \quad (6)$$

The term inside integral is integrated over all particles in the computational domain. The Biot-Savart relation written above is N-body problem that involves $O(N^2)$ evaluations. The calculation that involves $O(N^2)$ evaluations is called ‘direct computation’. It makes this method not practical because of large time consuming and high memory requirement. To accelerate the computation, the Fast Multiple Method (FMM) was employed. FMM is conducting velocity evaluation by grouping particles based on their position and the evaluation of inter-particles is bounded by the groups. In this approach, long distance inter-particles relation is approached by inter-groups relation so that it reduces amount of computation load. The detail method of FMM which was followed in this work can be found in [15].

To solve the diffusion term, particles strength exchange (PSE) introduced by Degond & Mas Gallic [3] was used to obtain the most accurate model. Using PSE, the Laplacian operator of the diffusion term is approximated by an integral operator:

$$\nabla^2 \omega(\vec{x}) \approx \frac{2}{\sigma^2} \int \eta(\vec{x} - \vec{x}') (\omega(\vec{x}') - \omega(\vec{x})) d\vec{x}' \quad (7)$$

With η for Gaussian distribution is defined as:

$$\eta(\vec{x}) = \frac{1}{2\pi\sigma^2} \exp\left(-\frac{|\vec{x}|^2}{2\sigma^2}\right) \quad (8)$$

The Equation (7) is discretized over particles and the calculation of time derivative of particles strength becomes:

$$\frac{d\Gamma_i}{dt} = \frac{2\nu}{\sigma_{ij}^2} \sum_{j=1}^N (A_i \Gamma_j - A_j \Gamma_i) \eta_{ij}(\vec{x}_i - \vec{x}_j) \quad (9)$$

Index i and j mean evaluated and influencing particles and index ij means average value of i and j associated to the property.

Predictor-corrector scheme is used to conduct time integration. For each iteration, the integration is divided into two step predictor and corrector.

- Predictor step: the further predicted position and strength of particles are obtained by integration of velocity using explicit Euler scheme:

$$\vec{x}_{n+1/2} = \vec{x}_n + \vec{u}_n(\vec{x}_n, \Gamma_n) \Delta t \quad (10)$$

$$\Gamma_{n+1/2} = \Gamma_n + \left. \frac{d\Gamma}{dt} \right|_n (\vec{x}_n, \Gamma_n) \Delta t \quad (11)$$

- Corrector step: velocity of particles is recalculated using new particles strength and taking average of velocity between predictor and corrector value and integrating the averaged velocity using explicit Euler scheme:

$$\vec{x}_{n+1} = \vec{x}_n + \frac{\vec{u}_n(\vec{x}_n, \Gamma_n) + \vec{u}_{n+1}(\vec{x}_{n+1/2}, \Gamma_{n+1/2})}{2} \Delta t \quad (12)$$

The result is vorticity field described by particles strength and position. The existence of vorticity field induces velocity slip on the body surface. This fact inspires concept of vorticity production [14] because of boundary condition enforcement. Physically, the velocity slip on surface must be vanish. The existence of induced velocity slip must be compensated by vorticity production of surface. Mechanism of the vorticity production is accommodated by introducing surface panels that produce vortex sheets γ (panels) and then vortex sheets are diffused into neighbourhood particles as illustrated in Figure 1.

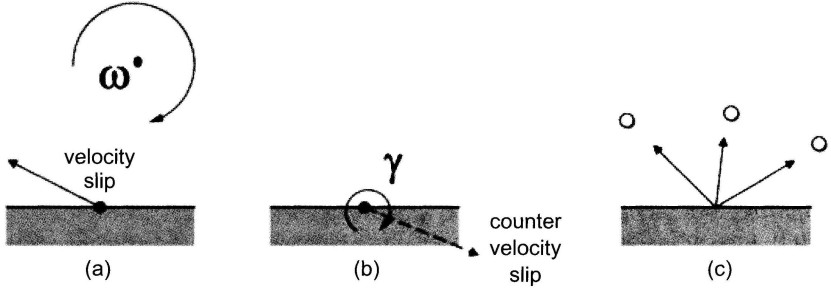


Figure 1: Schematic illustration of vorticity mechanism on surface: (a) vorticity distribution of flow field represented by single point vorticity ω induces velocity slip on a surface panel. (b) vortex sheet of a panel is produced to generate counter velocity slip in order that velocity slip is vanish. (c) produced vortex sheet on panel is diffused into surrounding particles.

The vortex sheet can be produced by inviscid solution of geometry panels governed by boundary integral equation as follow:

$$-\frac{\gamma(\bar{x})}{2} + \frac{1}{2\pi} \int_S \gamma(\bar{x}') \hat{n} \cdot \nabla \log |\bar{x} - \bar{x}'| d\bar{x}' = [(\bar{u}_{slip} - \bar{u}_b) \cdot \hat{s}] \quad (13)$$

The above equation describes that vortex sheet produced on certain panel represented by evaluated point $\gamma(\bar{x})$ is induced by vortex sheet remaining panels $\gamma(\bar{x}')$ to enforce specified velocity on \bar{x} to be $(\bar{u}_{slip} - \bar{u}_b) \cdot \hat{s}$, where \bar{u}_{slip} is velocity, \bar{u}_b is surface velocity and \hat{s} is parallel vector of surface. The integral equation is solved numerically using a common boundary element method to obtain $\Delta\gamma$ for each panel. The vortex sheet then needs to be diffused into particles. The appropriate vortex sheet diffusion scheme is given by [12] as follows:

$$\frac{d\Gamma_i}{dt} = \frac{\Delta\gamma}{\Delta t} ([\text{erf}(c)]_a^b) \left(\sqrt{4\nu t} \frac{1}{2} ([\text{ierfc}(s)]_c^d - [\text{ierfc}(s)]_e^f) \right)$$

$$a = \frac{(x_i + \frac{h_i}{2})}{\sqrt{4\nu t}}$$

$$b = \frac{(x_i - \frac{h_i}{2})}{\sqrt{4\nu t}}$$

$$\begin{aligned}
 c &= \frac{\left(x_i - \frac{b}{2} + \frac{h_i}{2}\right)}{\sqrt{4vt}} \\
 d &= \frac{\left(x_i - \frac{b}{2} - \frac{h_i}{2}\right)}{\sqrt{4vt}} \\
 e &= \frac{\left(x_i + \frac{b}{2} + \frac{h_i}{2}\right)}{\sqrt{4vt}} \\
 f &= \frac{\left(x_i + \frac{b}{2} - \frac{h_i}{2}\right)}{\sqrt{4vt}}
 \end{aligned} \tag{14}$$

where b is length of panel. Thus, the above equation is integrated numerically using explicit Euler scheme to obtain new particles strength contributed by body surface:

$$\Gamma_i^{n+1} = \Gamma_i^n + \Delta t \left. \frac{d\Gamma}{dt} \right|_{\text{surface}} (\mathbf{x}^{n+1}, \Gamma) \tag{15}$$

The last value of particles strength above is the final value of current time step and initial value for further time step

In certain step, because of the convection, particles arrangement in the flow field became irregular. In this situation, the density of particles is no longer uniform and vorticity distribution is no longer continuous. Unfortunately, the solution of PSE needs particles to be near regular arrangement to give appropriate accuracy. To accommodate this requirement, the particles will be relocated in regular arrangement in certain iteration. This step sometimes is called re-meshing. The detail technique of re-meshing employed here can be seen also in [4]. The re-meshing has N order of computation so that it increases inefficiency in computation time.

For moving body problem, the effect of surface velocity is included in boundary integral equation (13) determined by $\bar{\mathbf{u}}_b$. If surface velocity is specified as function of time, surface coordinates for next time step can be determined:

$$\bar{\mathbf{x}}_b^{n+1} = \bar{\mathbf{x}}_b^n + \Delta t \bar{\mathbf{u}}_b^n \tag{16}$$

With $\bar{\mathbf{x}}_b^{n+1}$ is body surface coordinate at $n+1$ time step. As summary, the calculation steps for each time step are given as follow:

- Define initial particles arranged around body specified by positions and strength
- Calculate initial vorticity production by solving Equation (13)-(15)

- Calculate particles velocity and increment of particles strength using (5) and (9)
- Conduct time integration using (10)-(12)
- Calculate surface coordinates for next iteration using (16)
- Calculate vorticity production for next iteration using (13)-(15)

The steps are executed iteratively until specified final iteration determining simulation time has been achieved.

Before computational code is executed, some parameters are necessary to be defined: interval time of each iteration Δt , smoothing parameter σ and interval space between particles h . Using Gaussian distribution, smoothing parameter can be related to interval space h as $\sigma = h$. PSE requires stability constraint as:

$$\frac{v\Delta t}{\sigma^2} \leq \phi \quad (17)$$

with

$\phi = 0.595$ for Euler explicit scheme

$\phi = 0.295$ for for the Adams–Bashforth 2scheme

Using predictor-corrector scheme, we use the lowest value of $\phi = 0.295$.

Force Calculation

Since vorticity distribution has been calculated, it is necessary to obtain fluid force for bounded flow. In vortex method, there are methods to calculate fluid force from known vorticity distribution [19], we choose the simplest one but robust enough called Impulse method given by formula:

$$\mathbf{F} = -\rho \frac{\int \bar{\mathbf{x}} \times \hat{\mathbf{e}}_z \omega dV}{dt} \quad (18)$$

with ρ = fluid density

where $\hat{\mathbf{e}}_z$ is normal vector of evaluation plane and dV is infinitesimal volume of particles. The integral term can be written in terms of summation over all particles strength as follow:

$$\mathbf{F} = -\rho \frac{\sum_{i=1}^N \bar{\mathbf{x}}_i \times \hat{\mathbf{e}}_z \Gamma_i}{dt} \quad (19)$$

Calculation of differential operator above can be conducted using common numerical method such as central difference or backward difference.

Simulations

Scenario of Simulations

The scenario of this numerical simulations follow Dickinson experiment [19]. He investigated force generation due to rapid rotation in flapping wing. As a result, he proposed a hypothesis to explain lift enhancement due to wake capturing. The hypothesis has not been confirmed by adequate flow visualization. However he investigated force behavior from amount of simulation modes. The simulated modes contain two part: down-stroke and upstroke. They refer to stroke direction of insect wing during flight. Each part is combination of translation and rotation.

Two modes of motion are followed in these numerical simulations. They have the same velocity profile and distinguished by angular velocity profile. The velocity profile is depicted in Figure 2. The negative velocity refers to direction moving from left to right as illustrated in Figure 4 and positive is the opposite. The differences of angular velocity between first mode (mode 1) and second mode (mode 2) are location of rapid rotation and magnitude of peak rotation. In the mode 1, rapid rotation occurs at the end of each stroke while in mode 2 it occurs at the beginning of the strokes. Mode 1 has larger magnitude of peak of rotation than mode 2. The starting angle of attack of mode 1 is 40 degrees and mode 2 is 130 degrees.

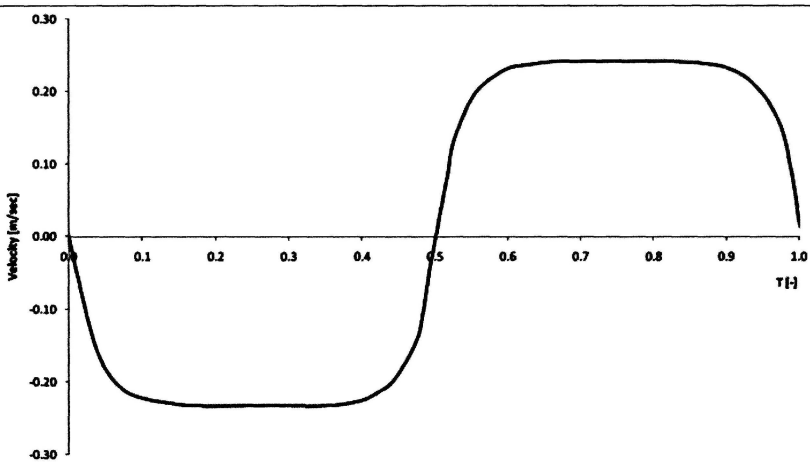


Figure 2: Velocity profile for the both modes (mode 1 and mode 2) as a function of normalized time (T) with respect to period . $0 \leq T < 0.5$ is down stroke and $0.5 \leq T \leq 1.0$ is upstroke

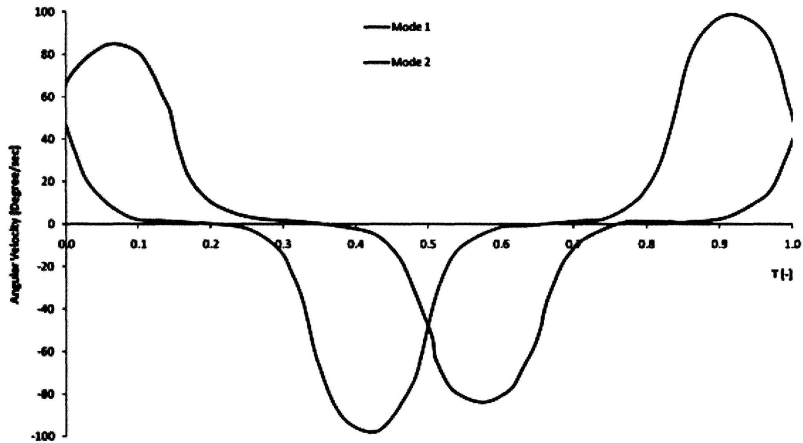


Figure 3: Angular velocity profile for mode 1 (blue) and mode 2 (red) as a function of normalized time (T) with respect to period. $0 \leq T < 0.5$ is down stroke and $0.5 \leq T \leq 1.0$ is upstroke. The both modes are distinguished by location of reversal stroke (shown by peak angular velocity) and peak magnitude of angular velocity

The illustration of the motions are depicted as follow:

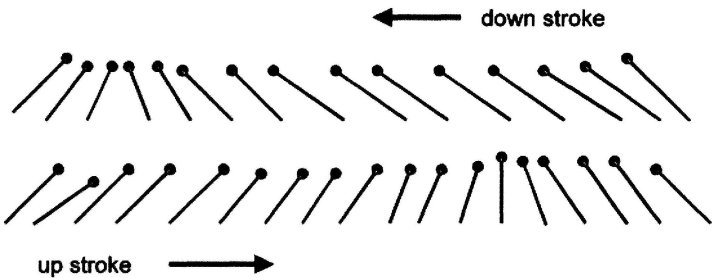


Figure 4: Illustration of motion of mode 1. Down stroke is moving from left to right (top) and upstroke is the opposite following the down stroke (bottom). The starting angle of attack is 40 degrees

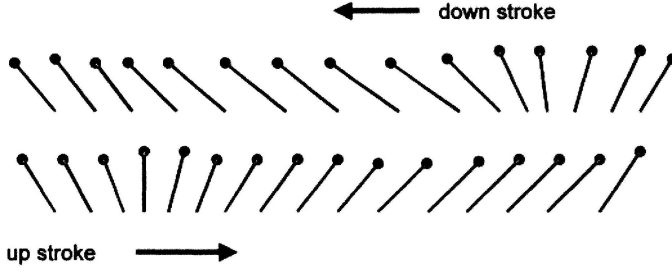


Figure 5: Illustration of motion of mode 1. Down stroke is moving from left to right (top) and upstroke is the opposite following the down stroke (bottom). The starting angle of attack is 130 degrees

In the experiment, [18] used wing model that the platform is similar to insect wing with span of 25 cm, area of 0.0167 m² (Aspect Ratio = 3.7) and thickness of 3.2 mm. The fluid medium was mineral oil with kinematics viscosity of 115 cSt and density of 0.88×10^{-3} . For detail measurement report, we suggest to refer to [18]. For numerical simulation, we follow such fluid parameters. Because of two dimensional consideration, we use flat plate as two dimensional wing model with assumed chord length of 6.68 cm (obtained from the wing area divided by its span) and thickness of similar to the experiment model. The chosen numerical parameter is ΔT of 0.004.

Results and Discussion

The numerical computation is performed for one period of the both modes simulation. The simulations produce data of particles strength as function of iteration step associated to quantity of time. From the data, we can obtain vorticity distribution using and fluid force using.

To discuss comparison of fluid forces between the experiment and recent calculation, the fluid forces are plotted in term of coefficient of lift and drag (C_L and C_D). The coefficients are defined as follow:

- Experiment (3D case)

$$C_L = \frac{2 \text{ Lift}}{\rho V_{peak}^2 A_{wing}} \quad (20)$$

$$C_D = \frac{2 \text{ Drag}}{\rho V_{peak}^2 A_{wing}} \quad (21)$$

Where V_{peak} is peak velocity and A_{wing} is wing area

- Numerical calculation (2D case)

$$C_L = \frac{2 \text{ Lift}}{\rho V_{peak}^2 c} \quad (22)$$

$$C_D = \frac{2 \text{ Drag}}{\rho V_{peak}^2 c} \quad (23)$$

where c is flat plate chord

The drag is considered as force opposite to flat plate moving direction and lift is perpendicular to the direction. In insect flight, C_D and C_L act as lift and propulsive force, respectively. The results of C_D and C_L calculation are depicted in Figure 6 for mode 1 and Figure 7 for mode 2, where they are being compared with results from Dickinson's experiment. For each plot, the down stroke occurs at $0 \leq T < 0.5$ and upstroke occurs at $0.5 \leq T \leq 1.0$.

Plots in Figures 6 and 7 show close agreement of the simulation results with experiment, except for the C_L of vortex method simulations contain more peaks than experiment. Peaks of lift and drag during rapid rotation can be appropriately captured as in Dickinson's experiment. On C_D plots (left of Figure 6 and 7), drag peaks are identified during rapid rotation. They occur at $0.3 \leq T \leq 0.5$, $0.8 \leq T \leq 1.0$ for down stroke and upstroke of mode 1, respectively. While for mode 2, they occur at $0.0 \leq T \leq 0.2$, $0.5 \leq T \leq 0.7$ for down stroke and upstroke, respectively.

From the results it is clear that the peaks timing depend on time of the rapid rotation. Therefore, the peaks are suspected to be directly related to the rapid rotation. As shown on the C_D plot, position and magnitude of peaks can be accurately predicted by the vortex method. However, on C_L plots, it seems

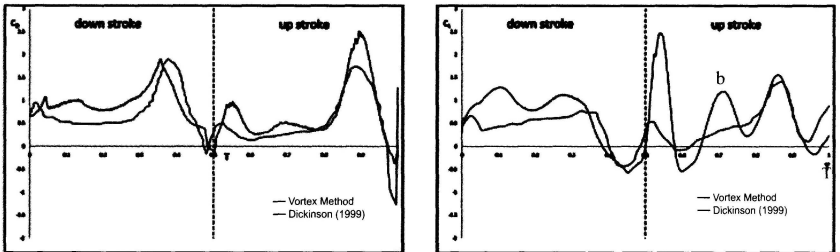


Figure 6: Comparisons of C_D (left) and C_L (right) between vortex method (blue) and Dickinson experiment (red) for mode 1. The coefficient of forces are plotted as function of normalized time respect to stroke period (T)

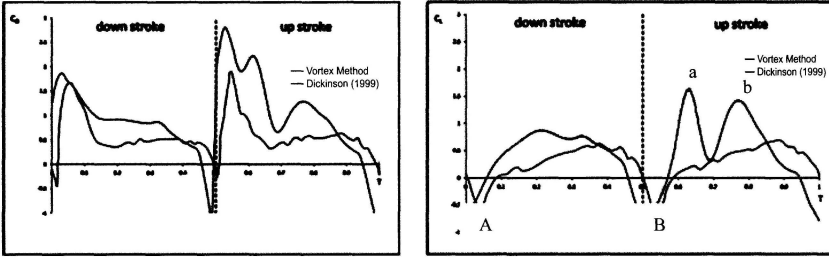


Figure 7: Comparisons of C_D (left) and C_L (right) between vortex method (blue) and Dickinson experiment (red) for mode 2. The coefficient of forces are plotted as function of normalized time respect to stroke period (T)

that there are additional peaks exist in vortex method simulation results that do not exist in experiment. The additional peaks will be discussed in the further part of this section.

There are several peaks shown in C_L plots (Figure 6 and 7). The lift peaks which correspond to the rapid rotation are marked by **A** and **B** on the C_L plots. Vortex method shows good accuracy in capturing peaks of **A** and **B**. According to the Dickinson explanation [18], the peaks of **A** and **B** are produced by wake capturing. This phenomenon causes the lift to immediately increase following the rapid rotation, if leading vortex from previous stroke is able to be captured by rotation. The increase in lift then produces top peaks of the lift. On the other hand, if no leading edge vortex is captured by rotation, lift will be triggered to decrease immediately.

Vorticity distributions during rapid rotation shown in Figure 8 and 9 (for the down stroke and upstroke of mode 1, respectively) reveal the relation between wake capturing and lift behaviour as explained by Dickinson. For down stroke (Figure 8) case, the inability of rotation to capture leading vortex (blue) leads to the decrease in lift and produces the bottom peak of lift (marked by **A**, right graph, Figure 6). Whereas as shown in Figure 9, the rotation during upstroke is able to capture leading edge vortex (red) effectively and, therefore, produces top peak of the lift (marked by **B** right graph, Figure 6).

Simulation of mode 2 shows further evidence about relation between wake capturing and the behaviour of lift. As shown on Figures 10 and 11, rotation during upstroke and down stroke captures no leading vortex because the both rotations occur at the beginning of stroke. As predicted, bottom peaks are produced following the rotation (marked by **A** and **B**, right graph, Figure 7). Above discussion shows good agreement between the vortex method simulation results and Dickinson's experimental results in revealing the wake capturing phenomenon.

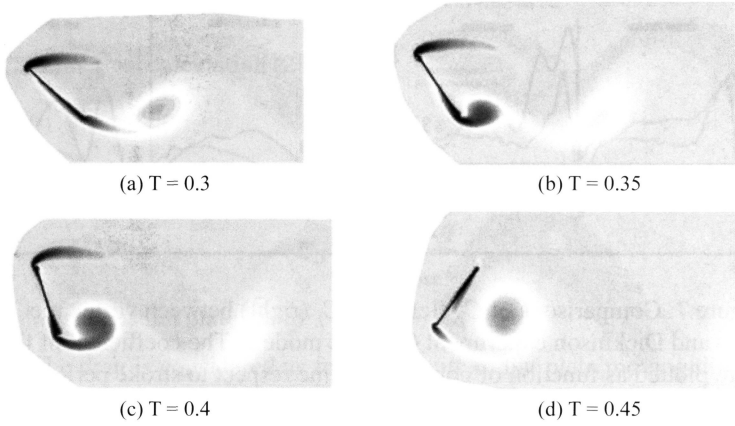


Figure 8: Vorticity distribution around flat plate of mode 1 at various T during the rapid rotation of down stroke. Blue colour indicates clockwise vorticity and the red is counter clockwise. Colour intensity shows magnitude of vorticity. The flat plate is rotating in clockwise direction and moving from right to left

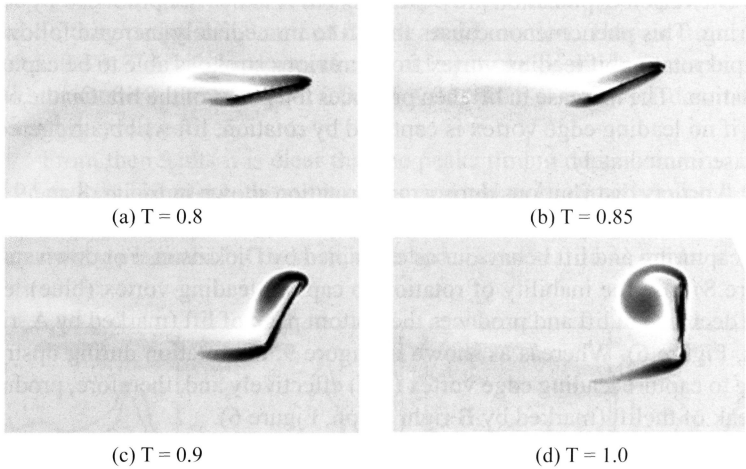


Figure 9: Vorticity distribution around flat plate of mode 1 at various T during rapid rotation of up stroke. Blue colour indicates clockwise vorticity and the red is counter clockwise. Colour intensity shows magnitude of Vorticity.

The flat plate is rotating in counter clockwise direction and moving from left to right

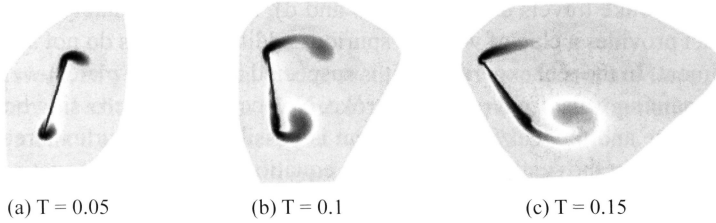


Figure 10: Vorticity distribution around flat plate of mode 2 at various T of down stroke around phase of the rotation. Blue colour indicates clockwise vorticity and the red is counter clockwise. Colour intensity shows magnitude of vorticity. The flat plate is rotating in counter clockwise direction and moving from right to left

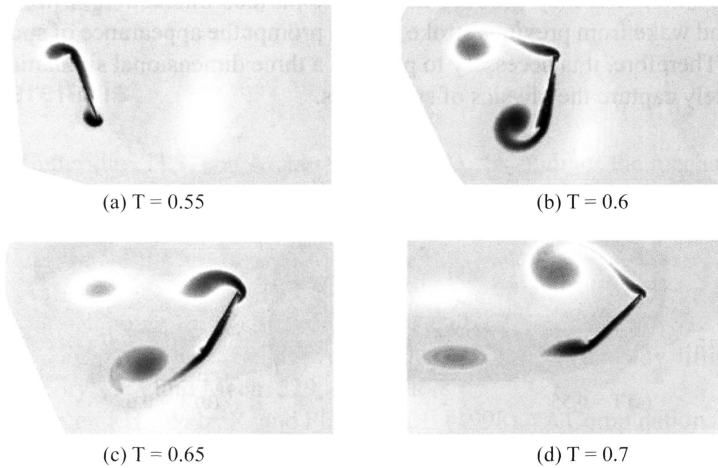


Figure 11: Vorticity distribution around flat plate of mode 2 resulted from vortex method at various T of down stroke around phase of the rotation. Blue colour indicates clockwise vorticity and the red is counter clockwise. Colour intensity shows magnitude of vorticity. The flat plate is rotating in clockwise direction and moving from left to right

As noticed before, C_l calculated from vortex method simulation contains additional peaks (as marked by a and b in Figure 6 and 7). By observing the vorticity plots, it is clear that these peaks do not correspond to the rotation. To investigate the additional peaks, we plot vorticity distribution when the peaks are occurring for mode 1 in Figure 12. Vorticity plots in the Figure 17 indicate that the additional peaks occur when the remaining wake from previous stroke (marked by dashed circle) is crossing with the flat plate as shown by (a) and

(c). As the wake travels downstream (b and d), lift is immediately decreased. This fact provides a clue of why the spurious additional peaks do not appear in experiment. In the real experiment, it is suspected that the flat plate never cross with remaining wake from previous stroke. No occurrence of crossing between the flat plate and the wake in experiment is possibly due to vortex stretching. As discussed in the section of governing equation, the vorticity equation used in simulation basically contains vortex stretching term, which disappears in two dimensional simulation. Whereas the real experiment involves vortex stretching because it is three dimension. It is suspected that vortex stretching in experiment makes wake in the previous stroke to disappear earlier than in the two dimensional simulation. Therefore, crossing between flat plate and the previous wake does not occur in the experiment. The explanation shows that vortex method is basically good enough for predicting properties of flows around a flapping wing. However, it is necessary to be noticed that the 2D vortex method simulation may produce additional spurious interaction between flat plate and wake from previous stroke, which prompt the appearance of spurious peaks. Therefore, it is necessary to perform a three dimensional simulations to accurately capture the physics of such flows.

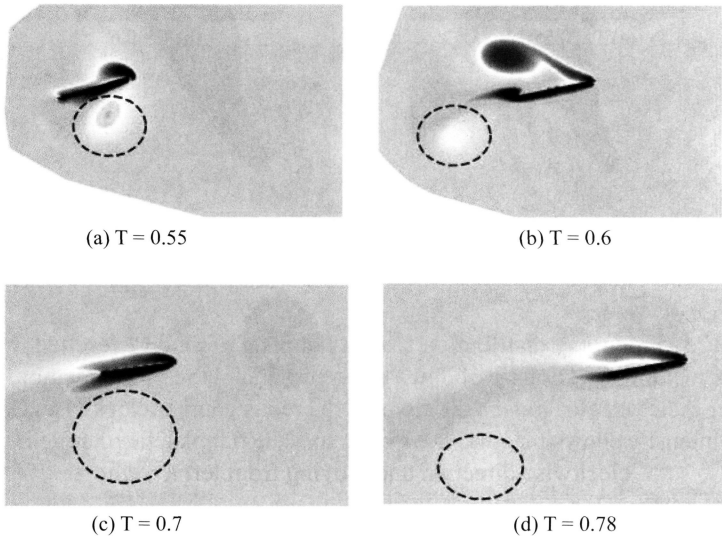


Figure 12: Vorticity distribution around flat plate of mode 1 at various T of upstroke when occur lift peaks (a and c) and thereafter (b and d). Blue colour indicates clockwise vorticity and the red is counter clockwise. Color intensity shows magnitude of vorticity. The remaining wake from previous stroke is marked by dashed circle

Conclusion

In this work, two dimensional vortex method is developed and used to simulate flows around a flapping wing. In general, the two dimensional simulations using vortex method are in good agreement with Dickinson's experiment, although the experiment was actually three dimensional. The developed vortex method has been shown to be able to reproduce the details flow field during the complex phase of rapid rotation. The C_D and C_L peaks due to rapid rotation are accurately predicted, in both magnitude and time of occurrences. In addition, the current simulation results provide evidence to the hypothesis proposed by Dickinson about the lift peaks generation due to wake capturing. Finally, the emergence of spurious peaks of lift, due to the disappearance of the vortex stretching terms in the two dimensional model, reveals the necessity of performing three dimensional simulation for investigating the details physics of flows around flapping wings.

References

- [1] Betteridge, D.S. and Archer, R.D. (1993). "A study of the mechanics of flapping flight", *Aeronaut. Q.* 25, 129-142.
- [2] Archer, R.D., Sappupo, J. and Betteridge, D.J. (1979). "Propulsive characteristics of flapping wings", *Aeronaut. J.* 83.
- [3] Ahmadi, A.R. and Widnall, S.E. (1986). "Energetics and optimum motion of oscillating lifting surfaces of finite span", *J. Fluid Mech* 162.
- [4] Guermont, J. and Sellier, A. (1991). "A unified unsteady lifting-line theory", *J. Fluid Mech.* 229, 427-451.
- [5] Tuncer, I.H., Walz, R. and Platzer, M.F. (1998). "A Computational Study of the Dynamic Stall of a Flapping Airfoil", *AIAA Paper* 93.
- [6] Isogai, K., Shinmoto, Y. and Watanabe, Y. (1999). "Effects of Dynamic Stall on Propulsive Efficiency and Thrust of a Flapping Airfoil", *AIAA Journal* 37.
- [7] Ramamurti, R. and Sandberg, W.C. (2001). "Simulation of flow about flapping airfoils using finite element incompressible flow", *AIAA J.* 39.
- [8] Chorin, A.J. (1973). "Numerical Study of Slightly Viscous Flow". *J. Fluid Mech* 57, 785-796.
- [9] Leonard, A. (1980). "Vortex Methods for Flow Simulation", *J. Comput. Phys.* 37, 289-335.
- [10] Degond, P. and Mas-Gallic, S. (1989). "The weighted particle method for convection-diffusion equations. I. The case of an isotropic viscosity; II. The anisotropic case", *Math. Comput.* 53.

- [11] Koumoutsakos, P.D. (1993). Direct Numerical Simulations of Unsteady Separated Flows Using Vortex Methods, California Institute of Technology.
- [12] Ploumhans, P. and Winckelmans, G.S. (2000). "Vortex Methods for High-Resolution Simulations of Viscous Flow Past Bluff Bodies of General Geometry", *Journal of Computational Physics* 165, 354-406.
- [13] Sepnov, A.J. (2009). Development of Three-Dimensional Vortex Element Method for High-Resolution Flow Simulation in Faculty of Mechanical and Aerospace Engineering, Institut Teknologi Bandung, Bandung.
- [14] Lighthill, M.J. (1963). *Introduction to Boundary Layer Theory*, (Oxford Univ. Press, New York).
- [15] Carrier, J., Greengard, L. and Rokhlin, V. (1988). "A Fast Adaptive Multipole Algorithm for Particle Simulations", *Siam J. Sci. Stat. Comput.* 9(4).
- [16] Eldredge, J.D. (2005). "Efficient tools for the simulation of flapping wing flows", in 43rd AIAA Aerospace Sciences Meeting and Exhibit, Reno, Nevada.
- [17] Eldredge, J.D. (2007). "Numerical Simulation of the Fluid Dynamics of 2-D Rigid Body Motion with the Vortex Particle Method". *J. Comput. Phys.* 221, 626-648.
- [18] Dickinson, M.H., Lehmann, F.O. and Sane, S.P. (1999). "Wing Rotation and the Aerodynamics Basis of Insect Flight", *Science* 284.
- [19] Noca, F. (1997). *On the evaluation of time-dependent fluid-dynamic forces on bluff bodies*, (California Institute of Technology).